Available online at www.sciencedirect.com
SCIENCE DIRECT®
ELSEVIER
Ad Hoc Networks xxx (2006) xxx–xxx
Ad Hoc Networks
www.elsevier.com/locate/adhoc

Improving routing performance in wireless ad hoc networks using cross-layer interactions

Erik Weiss [a,*], Guido Hiertz [a], Bangnan Xu [b], Sven Hischke [c], Bernhard Walke [a], Sebastian Gross [a]

[a] *Communication Networks, Faculty 6, RWTH Aachen University, Kopernikusstr.16, D-52074 Aachen, Germany*
[b] *SSC ENPS (Technologiezentrum), T-Systems, Am Kavalleriesand 3, D-64295 Darmstadt, Germany*
[c] *Deutsche Telekom AG, Friedrich-Ebert-Allee 140, D-53113 Bonn, Germany*

Received 29 November 2004; received in revised form 3 March 2006; accepted 17 March 2006

Abstract

This article presents a combined layer two and three control loop, which allows prediction of link breakage in wireless ad hoc networks. The method monitors the physical layer transmission mode on layer two and exploits the gained knowledge at layer three. The mechanism bases on link adaptation, which is used in IEEE 802.11a WLAN to select the transmission mode according to the link quality. The process of link adaptation contains information that is useful to predict link stability and link lifetime. After introducing the IEEE 802.11a Medium Access Control (MAC) and PHY layer, we present insight to the IEEE 802.11a link adaptation behaviour in multi-hop ad hoc networks. The link adaptation algorithm presented here is derived from Auto Rate Fallback (ARF) algorithm. We survey the performance gain of two newly developed route adaptation approaches exploding the prediction results. One approach is Early Route ReArrangement (ERRA) that starts a route reconstruction procedure before link breakage. Hence, an alternative route is available before connectivity is lost. Early Route Update (ERU) is a complementing approach that enhances this process, by communications among routing nodes surrounding the breaking link. The delay caused by route reconstruction can be significantly reduced if prediction and either of our new route discovery processes is used.

Keywords: Ad hoc network; Ad hoc routing; AODV; Link breakage prediction; Link adaptation; IPonAIR; ERRA; ERU; IEEE 802.11 MAC

1. Introduction

While it is increasingly important to be connected to the Internet world, the trend goes towards wireless solutions, providing mobile access to the Internet at high data rates. *Wireless Local Area Networks* (WLAN) like IEEE 802.11a operating at 5 GHz can

* Corresponding author. Tel.: +49 241 802 8575; fax: +49 241 802 2242.
E-mail addresses: erik.weiss@comnets.rwth-aachen.de (E. Weiss), hiertz@ieee.org (G. Hiertz), Bangnan.Xu@t-systems.com (B. Xu), Sven.Hischke@telekom.de (S. Hischke), walke@comnets.rwth-aachen.de (B. Walke), Sebastian.gross@comnets.rwth-aachen.de (S. Gross).

1570-8705/$ - see front matter © 2006 Published by Elsevier B.V.
doi:10.1016/j.adhoc.2006.03.003

support transmission rates up to 54 Mb/s. The high attenuation at 5 GHz limits the coverage area. One objective is therefore, to extend the coverage by establishing multi-hop routes. Since using wireless technology enables the user to be mobile, the network has to deal with effects introduced by a dynamically changing network topology.

High throughput and limited transmission range make WLAN systems adequate for areas with a high population density and users with the need for high data rates. Such places, like airports or fairgrounds, are called Hotspots. Covering large areas with WLAN is economically inefficient, since a considerable number of Access Point (AP) and routers would have to be deployed due to the limited transmission range. The AP density can be reduced by increasing the transmission power or enabling intermediate terminals to forward the data to users beyond the Access Point range. High transmit powers strain the batteries of the mobile devices and increase the exposure of operators to radio waves, along with their yet undetermined health risk (Fig. 1).

1.1. State of the art

Today's solution is to expand the fixed infrastructure using multi-hop connections. Mobility and fast changing topologies are addressed by ad hoc routing protocols, which can be subdivided into proactive and reactive protocols. Reactive protocols [4,17] request a route when needed, whereas proactive protocols [15,16] permanently maintain routes to all known network members that can be used on request, therefore minimizing packet delay. Reactive protocols avoid maintaining unneeded routes at the cost of a higher route discovery delay and packet delay. Therefore, hybrid approaches [18] have been developed to reach a trade-off between the reactive and proactive approaches.

However, in case of a route break, all routing approaches try to recover the connection. Most routing algorithms inform the source node, which in turn starts a completely new discovery process, thereby flooding the network with a large number of signalling messages. Some routing protocols perform a local route discovery [4] around the breakage to limit the flooding. Moreover, all aforementioned approaches solely only react when the link is already broken. This leads to a high number of lost packets as well as increased route rediscovering and packet delay.

The new strategy proposed in this paper is not to wait until the link breaks but to act in advance. Based on link adaptation information we predict the link state and start to rearrange the route before the link is interrupted. Lower layers, especially the link adaptation (LA), provide information that allows predicting the link conditions. We present Early Route ReArrangement (ERRA) and Early Route Update (ERU), two new route rearrangement protocols based on link prediction. Since the two presented approaches prevent unnecessary signalling, avoid packet loss and minimize packet delays, both use the ad hoc network capacity more efficiently than existing protocols.

A similar work based on legacy IEEE 802.11 was presented in [2], although the prediction approach presented in paper employs the received signal strength to estimate the likelihood of a link interruption. The approach in [2] is limited to informing the route's source about expected route breaks. The

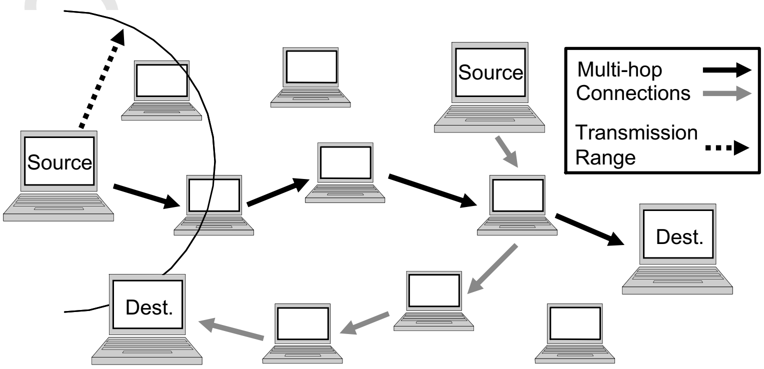

Fig. 1. Wireless ad hoc network.

source node has to act upon this information and the source node starts flooding the network to update the route using standard routing algorithms.

Our approach combines the idea of local route rearrangement on layer three and link prediction at layer two. We propose a prediction algorithm that takes advantages of the link adaptation (LA) actions. We use the link adaptation like a pre-processing function for the evaluation of channel conditions.

The remaining parts of the paper are organized as follows: we start with a brief survey of IEEE 802.11. The link adaptation fundamentals are covered in Section 3, followed by a discussion on how the link adaptation supports the necessary prediction information in Section 4. Simulations provide further information on the efficiency of the presented link adaptation. After giving a brief description of the ERRA and ERU signalling procedures, we highlight the benefits of the new protocols in Section 5. In Section 6 we present the simulation results of our new route rearrangement protocols ERRA and ERU. The last two sections conclude our consideration and discuss further research topics.

2. IEEE 802.11a medium access control

The IEEE 802.11a standard describes an OFDM PHY layer at 5 GHz. The Medium Access Control (MAC) layer is equal to IEEE 802.11b and legacy IEEE 802.11. IEEE 802.11a mainly introduces higher data rates [1,3]. IEEE 802.11a offers eight coding and modulation schemes, so called PHYModes (cf. Table. 1). The MAC protocol used in IEEE 802.11 is called Distributed Coordination Function (DCF). IEEE 802.11 furthermore describes a Point Coordination Function (PCF). The PCF is used for centrally controlled access. To our knowledge, it is has never been implemented by any vendor. The DCF is based on carrier sense multiple access with collision avoidance (CSMA/CA). As mobile nodes (MNs) are not able to monitor the air interface while transmitting, the DCF uses backoff and request to send/clear to send (RTS/CTS) mechanisms to avoid collisions due to the "hidden station" problem. Details of the IEEE 802.11 MAC protocol are given in [3].

Table 1
PHYMode dependent parameters

Data rate (Mb/s)	Modulation	Coding rate (R)	Data bits per symbol
6	BPSK	1/2	24
9	BPSK	3/4	36
12	QPSK	1/2	48
18	QPSK	3/4	72
24	16-QAM	1/2	96
36	16-QAM	3/4	144
48	64-QAM	2/3	192
54	64-QAM	3/4	216

2.1. IEEE 802.11a transmission modes

The IEEE 802.11a standard does not specify any rules for selecting the transmission mode. Each vendor implements a proprietary link adaptation method. The first four bits within each packet preamble specify the PHYMode chosen for coding the data payload. Higher transmission modes are capable of delivering higher data rates, but need a considerably higher carrier-to-interference ratio (C/I), thus limiting the bridged distance (cf. Figs. 2 and 3). In Table. 1 all available modes are listed with their respective maximum data rate, applied code rate and bits per OFDM symbol [1,3].

Due to the channel attenuation the C/I secedes as the distance between transmitter and receiver increases. Thus, different areas can be dependably covered with each PHYMode (cf. Fig. 2). IEEE 802.11a allows stepping down the transmission mode when the channel quality is decreasing, e.g., due to a rising distance between source and destination or in case of growing interference (cf. Fig. 3).

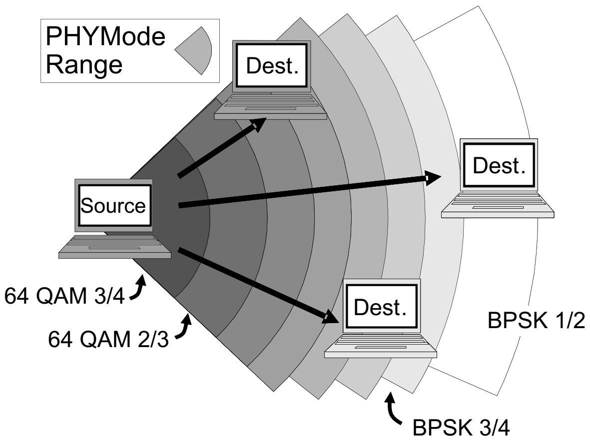

Fig. 2. PHYMode range.

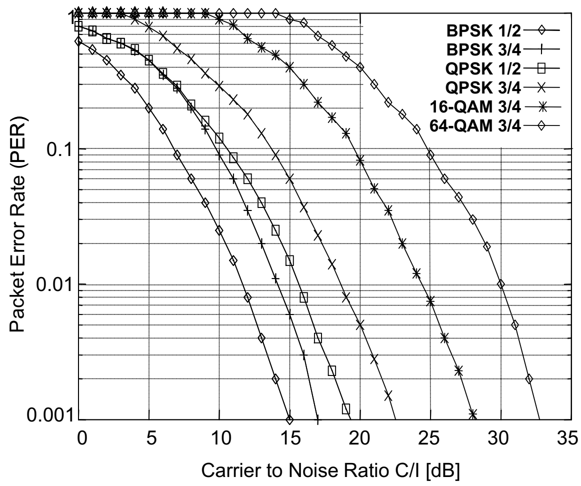

Fig. 3. Packet error rate versus C/I.

The IEEE 802.11a protocol allows choosing of an individual PHYMode for each connection and each data packet. Every terminal attempts to determine the PHYMode providing the best balance of throughput to packet error rate (PER). The Chair of Communication Networks, RWTH Aachen University [12] has developed a simulation tool to investigate IEEE 802.11a/e/g together with a complex IP layer. The simulation tool makes use of a two-path propagation model over a reflecting surface [1,12] as the physical channel model. It combines calculated C/I with the measured values, Fig. 3 shows exemplarily some values [13]. The results from our simulation environment presented in Fig. 4 evaluate the maximum throughput per PHYMode for a packet size of 2000 B. Since the 802.11 MAC handles small sized packages very inefficiently, our simulation results present a best-case scenario. The envelope of the throughput results is formed by the upper bound of all PHYModes and represents the optimum balance of PER and throughput. Since terminals in a real system cannot distinguish between signal power and interference power, it is impossible to measure the detailed C/I for each packet: Hence, each terminal only detects a certain local power level.[1]

There are two ways to estimate the signal-to-noise ratio: Terminals can either measure the interference power within transmission pauses, or count the successfully received and lost packets. The latter one is not intricate to implement as described in Section 3. The ratio between received and lost packets, combined with the measured packet error rate (PER) per PHYMode, leads to the prevailing C/I [12,13]. The IEEE 802.11a/g/e network simulator bases on PER versus carrier-to-interference ratio measurements [12] shown in Fig. 3. Higher transmission modes are capable of delivering higher data rates. But nevertheless, they also need a remarkably higher C/I. Decrease of the channel quality has several reasons, like fading, obstacles and interference. Fig. 4 presents the maximum achievable data throughput of IEEE 802.11a with the DCF and RTS/CTS handshake.

As presented in Fig. 4 802.11a carries up to 36 Mb/s when utilizing the 64-QAM 3/4 PHYMode. To improve the performance, a simple but efficient approach has been developed. After having successfully sent a predefined number of packets the LA of the transmitting station, steps up to a faster data rate. If a certain number of packets is lost later on, a lower transmission mode is used. This link adaptation algorithm is called Auto Rate Fallback (ARF). Further details can be found in [9]. However, this algorithm is instable. Even if LA has found an optimum transmission mode it will try to switch to a less robust but higher PHYMode leading to an increased packet error. Some other LA approaches have been presented in [10,11]. They outperform ARF but require changes to the IEEE 802.11 standard [3].

3. Link adaptation for multi-hop ad hoc network

Since IEEE 802.11 does not define any rules for an internal link adaptation (LA), each vendor implements a proprietary LA. Our prediction approach and route rearrangement protocols rely on the behaviour of the LA, thus it is mandatory to specify the used LA. Independently from the flavour of the LA, all algorithms are based on a similar principle that with degrading channel conditions a lower but more robust PHYMode is chosen (or a higher but less robust one, when the channel conditions improve).

To evaluate the performance of 802.11 MAC in a wireless multi-hop ad hoc network, our simulation tool has been extended with a fast and efficient LA. The developed LA can be described as an

[1] This is the reason why routing protocols based on signal strength stability operate on an uncertain basis. The received signal strength changes very dynamical due to the burstiness of the traffic.

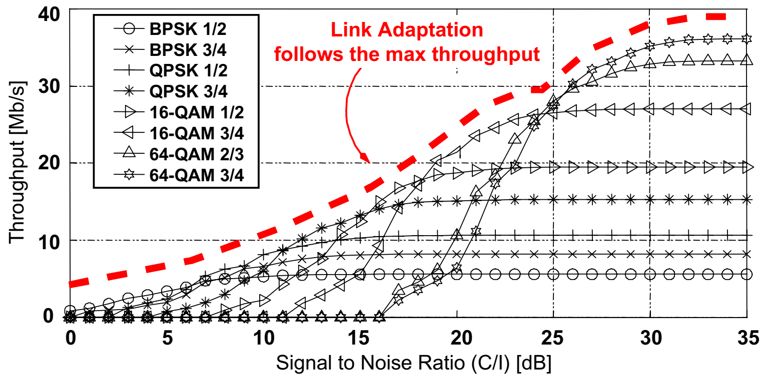

Fig. 4. Reachable throughput per PHYMode.

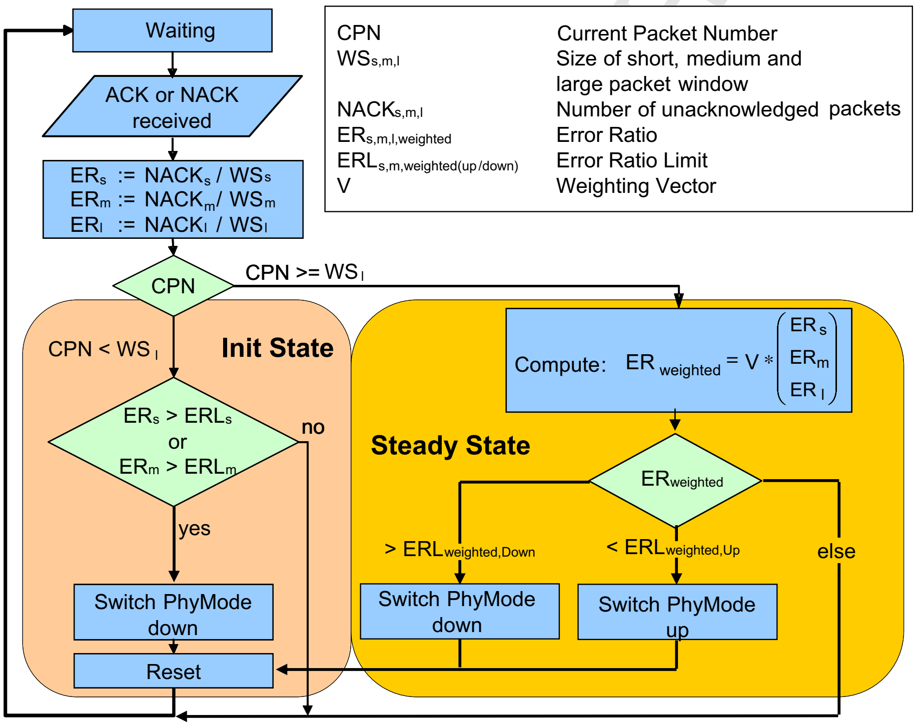

Fig. 5. Link adaptation working principle.

enhanced version of the Auto Rate Fallback (ARF) [9] protocol. Fig. 5 shows the functional principle of our LA algorithm. One LA instance serves one destination only. The implemented version addresses the following design specifications.

Fast reaction on channel condition changes is one of the major requirements for a LA, though slow variation must be considered as well. To fulfil these requirements, our LA contains three different lists (packet windows, PWs) of the sizes 5, 10 and 25 to store the PHYModes used in the past, along with the information whether the respective packet has been acknowledged or not. The parameter values are the result of various tests to find optimized parameters for a large range of possible test scenarios. As these PWs store short, medium, and long-term information they are referred to as short (PW_s), medium (PW_m) and long (PW_l) packet window (cf. (3.1)). The different window sizes (WSs) are labelled as short WS_s, medium WS_m, and long WS_l. The latest packet determines the current packet number (CPN):

$$
\begin{aligned}
\mathrm{PW_s} &= \{P_{\mathrm{CPN}}, P_{\mathrm{CPN}-1}, \ldots, P_{\mathrm{CPN}-\mathrm{WS_s}}\},\\
\mathrm{PW_m} &= \{P_{\mathrm{CPN}}, P_{\mathrm{CPN}-1}, \ldots, P_{\mathrm{CPN}-\mathrm{WS_s}}, \ldots, P_{\mathrm{CPN}-\mathrm{WS_m}}\},\\
\mathrm{PW_l} &= \{P_{\mathrm{CPN}}, P_{\mathrm{CPN}-1}, \ldots, P_{\mathrm{CPN}-\mathrm{WS_s}}, \ldots,\\
&\qquad P_{\mathrm{CPN}-\mathrm{WS_m}}, \ldots, P_{\mathrm{CPN}-\mathrm{WS_l}}\}.
\end{aligned} \tag{3.1}
$$

Each entry $P_i \in \{0,1\}$ has two states: either the packet was transmitted successfully ($P_i = 0$) or the packet was not acknowledged ($P_i = 1$). Our procedure permanently calculates the ratio of successful to unsuccessful transmissions (error ratio k, ER_k) for each PW_k (cf. (3.2)).

$$
\mathrm{ER}_k = \frac{1}{\mathrm{WS}_k} \sum_{\mathrm{CPN}-\mathrm{WS}_k}^{\mathrm{CPN}} \mathrm{PW}_k, \quad k \in \{\mathrm{s}, \mathrm{m}, \mathrm{l}\}. \tag{3.2}
$$

Eq. (3.2) shows how the ER_k is calculated. Whenever a packet is transmitted immediately after the PHYMode has been changed or if the link has been idle for a certain period of time the respective LA instance is reset. All packet windows are deleted (entries are set to zero) and the new packet is labelled as the first one (CPN is set to 1).

Our LA algorithm is designed to differentiate two states: the '*Init State*' and the '*Steady State*'. After the creation or the reset of a LA instance, the LA starts in the '*Init State*' (cf. Fig. 5). When a new link is established it is important to find an appropriate PHYMode before the IEEE 802.11 protocol starts discarding packets. Otherwise, the IEEE 802.11 retry counter may expire [3]. Therefore, the LA remains in '*Init State*' until all lists PW_k are filled. In this '*Init State*' the LA converges fast from the initial PHYMode to the actual link conditions, since only $\mathrm{PW_s}$ and $\mathrm{PW_m}$ are considered for the decision on switching to another PHYMode. Each PW_k is associated with a certain error ratio limit (ERL_k). When the LA procedure operates in the '*Init State*' and the error ratio within $\mathrm{PW_s}$ or $\mathrm{PW_m}$ exceeds the corresponding ERL, the PHYMode is immediately decreased (cf. (3.4) and (3.5)). The $\mathrm{WS_s}$ has to be carefully selected. During our studies presented here, the initial PHYMode was kept equal to the PHYMode used for layer three broadcast transmissions. Therefore, all layer three control packets are sent using QPSK 3/4. To further enhance the LA procedure, after entering the '*Init State*' the LA instance evaluates current or previous backwards links if available. If a backwards link exists and its PHYMode is lower than the initial default PHYMode, the PHYMode of this backwards link is used as the initial one, see Fig. 6. Node A transmits using BPSK 1/2 to node B. Node A has already adapted the PHYMode to find the best suited one. Hence, node B uses the same coding scheme of node A as the initial PHYMode. This behaviour is based on elevated probability that both directions have comparable propagation conditions. This educated guess is used to improve the starting point for LA, as described above.

Once all lists have been filled the LA instance switches to the '*steady state*' where all lists are considered for further calculations. To differentiate between long term and short term changes the three $\mathrm{PW_{s,m,l}}$ are weighted using a weighting vector $\vec{V}$ (see (3.3)). The weighting vector contains a weight v_i for each PW_k with $v_i \in \Re \cap [0,1]$.

$$
\vec{V} = \begin{pmatrix} v_1 \\ v_2 \\ v_3 \end{pmatrix} \quad \text{with } v_i \in \Re \cap [0,1] \text{ and } \sum_i v_i = 1. \tag{3.3}
$$

The current PHYMode is taken as the current optimum as long it remains in a predefined range. The

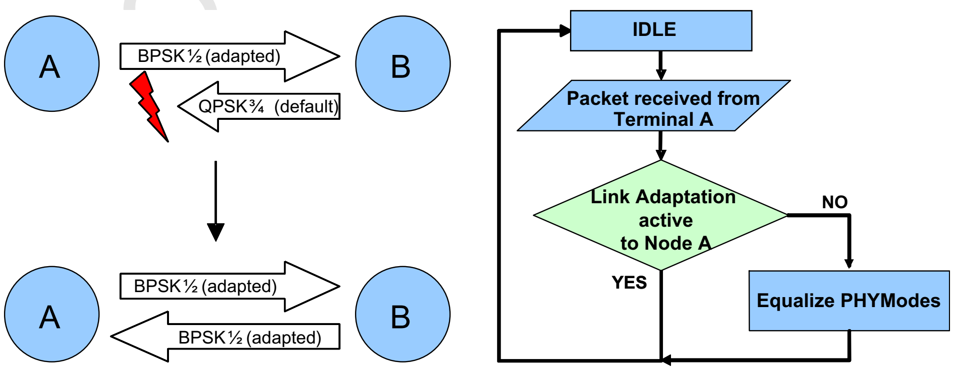

Fig. 6. Considering the bidirectional case.

bounds of this range are given by $ERL_{Weighted,UP}$ and $ERL_{Weighted,DOWN}$. If the weighted error ratio falls below $ERL_{Weighted,UP}$ the PHYMode is increased and vice versa when the weighted error ratio arises over $ERL_{Weighted,DOWN}$ the PHYMode is decreased. Our LA switching conditions are summarised in Eq. (3.4) and (3.5).

$$\text{Switching}_{\text{DOWN}} = \begin{cases} (ER_s > ERL_s) \cup (ER_m > ERL_m) \\ \quad \text{for } CPN < WP_l, \\ \begin{pmatrix} v_s \\ v_m \\ v_l \end{pmatrix} \otimes (ER_s; ER_m; ER_l) > ERL_{Weighted,DOWN} \\ \quad \text{for } CPN \geqslant WP_l. \end{cases} \tag{3.4}$$

$$\text{Switching}_{\text{UP}} = \begin{cases} \text{non-switching up in } \textit{Init State} \\ \quad \text{for } CPN < WP_l, \\ \begin{pmatrix} v_s \\ v_m \\ v_l \end{pmatrix} \otimes (ER_s; ER_m; ER_l) < ERL_{Weighted,UP} \\ \quad \text{for } CPN \geqslant WP_l. \end{cases} \tag{3.5}$$

To be able to react to rapidly changing channel conditions, PW_s should be highly weighted. For the simulation results presented here the weights are set as follows: $\{v_1 = 0.5; v_2 = 0.3; v_3 = 0.2\}$. This means PW_s weighted with 50%, PW_m with 30%, and PW_l with 20%.

The right choice for the WSs is a key requirement for a sufficient LA operation. High data rate connections having small packets need larger WSs than a moderate data rate connection with large packets. Therefore, an additional function at each terminal has to measure the data packet rate per link and to choose the packet window sizes independently for each link. However, in addition to the packet rate, the WS_s has to be defined small enough to avoid expiring the IEEE 802.11 retry counter [3]. Therefore, during our studies a PW_s of five packets has been used to prevent packet loss in the '*Init State*'.

However, optimizing LA algorithm is out of the scope of this article. Our focus here is to increase ad hoc routing performance using cross-layer information in support of ERRA and ERU. Nevertheless, giving a detailed description of the LA is necessary since they are none standardized LAs. Our LA turns out to be a suitable choice as basis for a prediction algorithm. The next section shows the LA behaviour and performance.

4. Link adaptation behaviour

We use two scenarios to present the stability and performance of the LA developed. The velocities used in our simulation are applicable in cases such as a walking person or a slowly moving vehicle. Faster speeds would mean frequent changes of links and thus result in an inconstant link quality. Vehicle

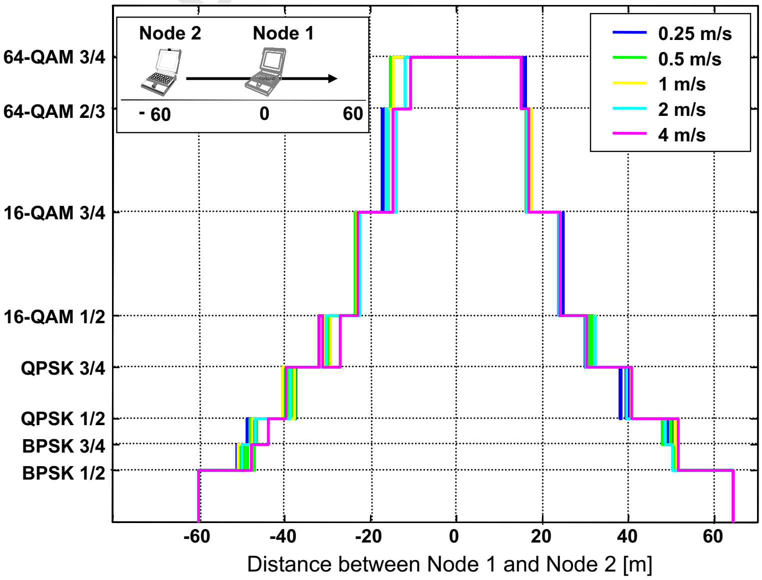

Fig. 7. Throughput results of node 2, under different velocities.

based scenarios do not provide a promising application for stand-alone wireless local area networks.

First, we investigated a basic scenarios comprising two nodes. One node remains immobile. We place the fixed node at the point of origin. The second node is placed at a distance of 60 m, it moves straight towards the fixed node and stops after leaving the range of node 1. The aim of this setup is to gain insights into the detailed LA reaction and to observe the stability of the LA. The scenario is shown in Fig. 7 on the upper left corner. Node 1 transmits to node 2. The offered data rate was 100 kb/s constant-bit-rate (CBR) with a packet size of 512 B. Both nodes transmit with a power of 100 mW. The propagation coefficient of the physical model was assumed to be $\gamma = 3.0$ [1]. Realistic values for γ are between 2 (free-space propagation) and 5 (strong attenuation, e.g., because of city buildings). The simulation is repeated with varying speeds of node 2.

Fig. 7 presents the used PHYModes for packets transmitted from node 1 to node 2. The adaptation steps can be observed for velocities from 0.25 m/s up to 4 m/s. It shows that the link adaptation is capable of swiftly adapting the PHYModes. An influence of the velocity can be stated for 2 m/s and 4 m/s, whereas all other velocities show roughly similar adaptation behaviour. The LA needs longer to increase the PHYMode when the destination station approaches faster. The downward curves are almost identical in all cases showing that the decreasing quality of the link is detected comparably at any simulated speed.

5. Predicting link breakages

Continuous switching down of PHYModes is a hint for the network layer that the link may break soon. This information triggers the routing algorithm instance to reconsider the route and to adapt it according to the emerging situation. Being able to predict a link breakage has large benefits. Common routing protocols react after a link is broken, while using LA information our solution acts before the breakage occurs. The channel dump in Fig. 12 presents three LA behaviour examples extracting typical *downstairs-patterns*. The next step is to evaluate the relation between a *downstairs-pattern* and a possible route break.

5.1. The rating function

To investigate the LA behaviour and detect *downstairs-patterns* automatically, we defined a rating function RF(t) shown in Fig. 8. The RF(t) ranks the importance of PHYMode changes in relation to a breakage (cf. Fig. 8). A change from BPSK 3/4 to BPSK 1/2 (value 7) for example is more important for the breakage prediction than switching from 16-QAM 3/4 to 16-QAM 1/2 (value 3).

An important issue in the context of detection rate and false alarms is the history of the previous LA decisions. A detection threshold ($DF_{\text{threshold}}$) has to be determined in accordance to these information. The time window taken into account for threshold determination is named detection interval (DI). We sum up all ratings within a limited timeframe. Switching down is valued as negative, switch-

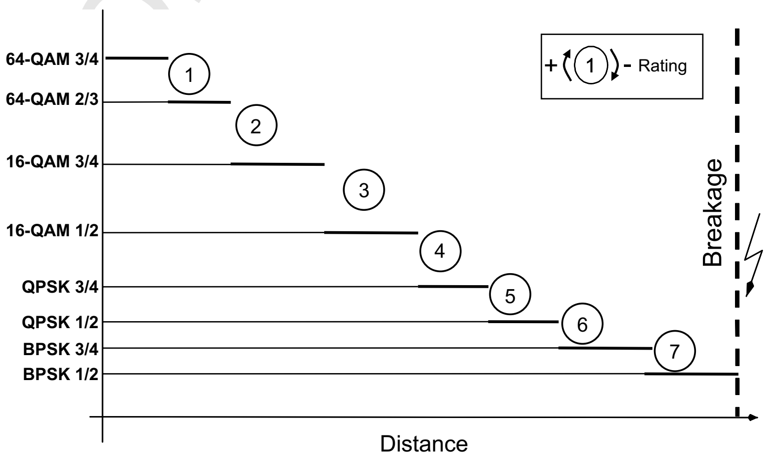

Fig. 8. Rating function.

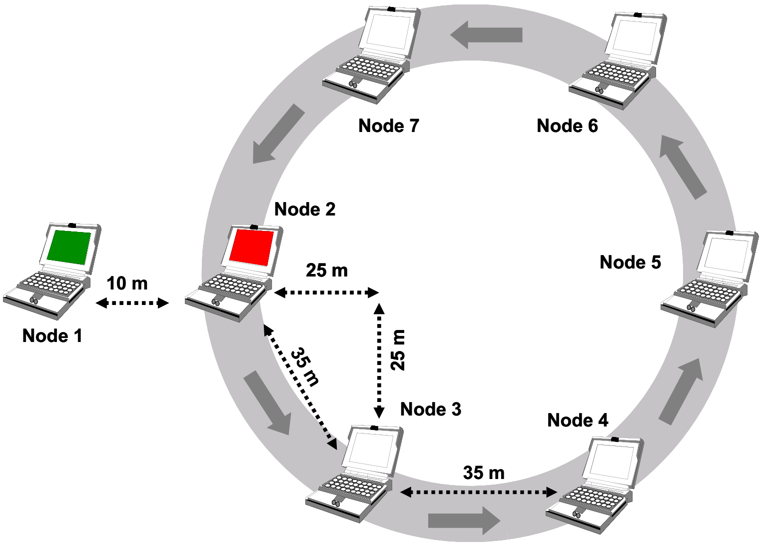

Fig. 9. Idealised demonstration use case.

ing up as positive. Whenever a LA algorithm advises the MAC to use the last feasible PHYMode (BPSK 1/2), the prediction method uses the RF(t) to measure the link behaviour in the elapsed timeframe. The prediction algorithm sums up all valuations done prior to the step to BPSK 1/2. To judge the shape and speed of the downstairs pattern the sum-up results are compared to a certain detection threshold.

We introduce a small scenario to show an idealised use case for our breakage prediction and route rearrangement algorithms. The scenario is presented in Fig. 9[2] and includes seven nodes. It explains the major advantages of breakage prediction based on the LA for ad hoc routing. The source node 1 (green) is stationary. The other nodes are arranged in a circle uniformly distributed with a distance of 35 m. Node 1 is 10 m apart from the circle. Node 2 is the red destination node and circularly moving with the other nodes at a predefined speed of 1 m/s. The offered traffic stream has a constant bit rate of 100 kb/s. The packet size is 512 B and simulation time is 210 s. The circular setup was chosen to minimize simulation time and number of nodes involved.

The movement causes all established routes to degrade in link quality and eventually (without prediction) to break between node 1 and its next hop partner. Those breakages accompany packet loss and rerouting. Our results in Fig. 10 show that routes using standard AODV experiences a long period of time using BPSK 1/2 before the link ultimately breaks. After the actual route break, resulting in a loss of data packets, AODV reroutes and consequently the link quality increases again.

Breakage prediction enables the routing algorithm to start this rerouting process as soon as BPSK 1/2 is reached. The new route is found and can be engaged long before the actual route break occurs. The link quality is considerably improved when using breakage prediction and more stable routes are found. Furthermore, in the prediction based case no link breaks or packet losses occur.

Besides the basic evaluations, we stress the LA and prediction with a larger scenario to investigate the LA performance under more realistic traffic conditions. A second setup shown in Fig. 11 presents an ad hoc network containing 40 nodes. Except for the source and destination node of the three routes investigated here, all nodes move according to the Random Waypoint Model (RWP) [7]. However it is important to note that a RWP [7] scenario is a worst case for breakage prediction. Any predication is based on the assumption that a measured development continues in the future. Human movement in real life situation is for the most part goal-oriented. Therefore, under normal circumstances the link degradation follows the assumption and can be predicted with certain reliability. A RWP mobil-

[2] For interpretation of colour in this figure, the reader is referred to the web version of this article.

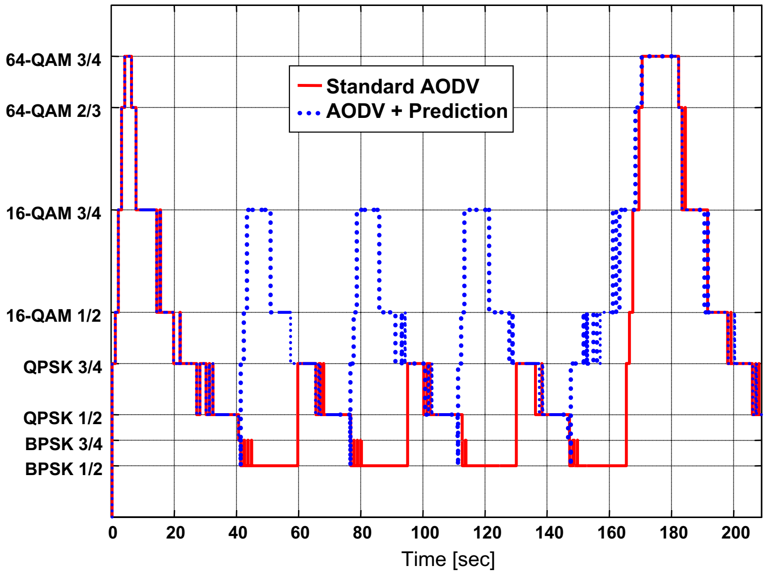

Fig. 10. Benefits of prediction based routing.

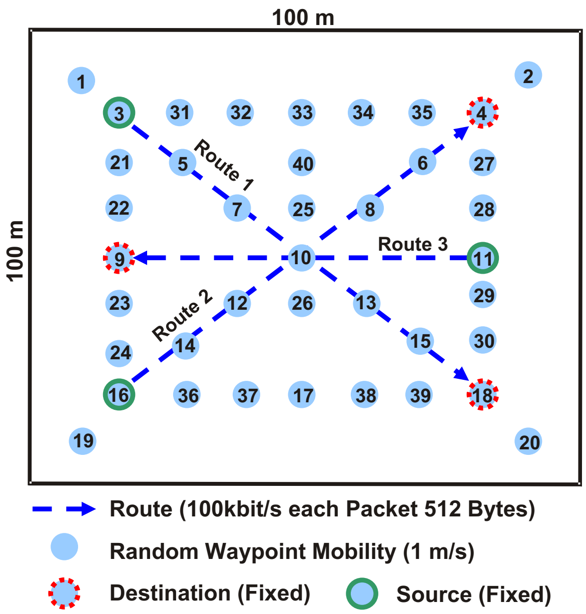

Fig. 11. Ad hoc example.

ity model generates just the opposite of a goal-oriented behaviour. We use it in our investigations because it is the commonly used model to simulate movement behaviour for ad hoc networks and to assure the superior properties of ERRA and ERU even under worst-case conditions.

Each source node generates a traffic of 100 kb/s using a constant-bit-rate (CBR) traffic generator. The packet size is 512 B. The window sizes for the LA algorithm are set to $WS = \{WS_s = 5;\ WS_m = 10;\ WS_l = 25\}$. Fig. 12 presents the corresponding LA behaviour for the source with the node number three. Due to the mobility of the nodes, the number of hops and the forwarding nodes change constantly. Fig. 12 presents the PHYMode of all packets successfully sent by node 3. Node 3 as a source node is not mobile. Several route breakages can be observed along the routes (dashed lines). Thus, Fig. 12 presents the link breaks between station 3 and its respective next hop-partner. Of course, link breaks may occur on different links along the whole route, too. Each link breakage results in a new route discovery process.

We emphasise three particular situations in Fig. 12 indicating a typical LA behaviour in advance to a link failure. Breakages between node 3 and its next hop on the route are marked with a dashed vertical line. The node speed was set to 1 m/s for all moving nodes. Fig. 12 contains three subfigures. The upper figure presents the PHYModes adjusted by the link adaptation process from 650 s to 1350 s after the beginning of the simulation. Our LA algorithm switches several times to faster PHYModes when link conditions improve and the other way when conditions decrease. Three typical situations are highlighted (by grey blocks) and presented in detail below. Subplot Fig. 12(a) presents the typical channel pattern that can be observed in

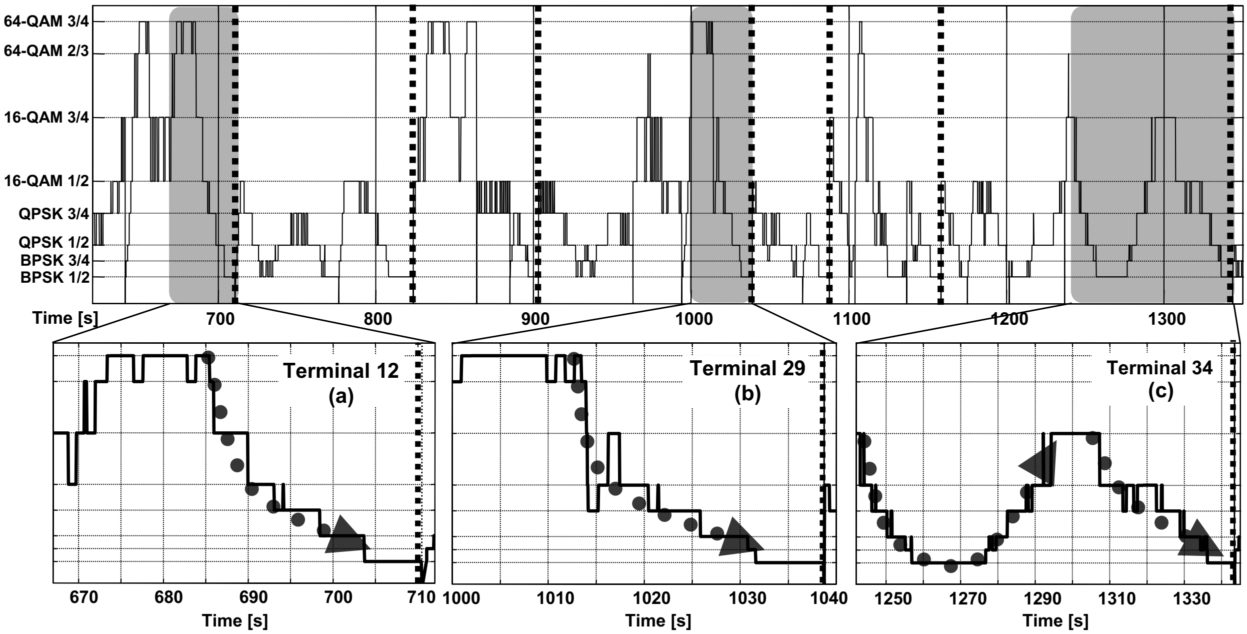

Fig. 12. PHYMode dependent channel monitoring for multi-hop ad hoc networks.

advance of a link breakage. Fig. 12(b) highlights the time interval [1000 s; 1040 s]. It presents an interfered pattern, although the pattern can be still identified. In addition, the third subplot Fig. 12(c) extracts one of the challenges our prediction algorithm has to deal with. The pattern of the first part of subplot (c) suggests an upcoming breakage. However, no break occurs in the highlighted situation. On the contrary, our LA algorithm increases the PHYMode. This can be observed several times and depends on the mobility model used. For instances, with RWP mobility the node moves away, reaches its drawn point and returns. Therefore, the link quality decreases when moving to the far point and increase on the way back again. This is depicted in the first part of subplot (c).

As expected the link quality decreases with increasing distances. Our LA procedure adapts whenever necessary to avoid a connection interruption. Based on this behaviour, we are able to predict a link breakage.

Fig. 13 presents a histogram depicting the influence of the detection interval and the detection threshold on the detection rate. The histogram shows the detection rate for the scenario presented in Fig. 11. With an increasing detection interval the detection rate rises. Based on Fig. 13 one can also state that a detection threshold lower than −22 is not suitable. Applying a threshold of −18 and a detection interval of around 40 s, allows predicting 70% of all occurring breakages. Apart from the detection rate, the number of needless route rearrangements is an important measure to evaluate the prediction performance. Fig. 14 presents a histogram visualizing the percentage of correctly detected breaks. Under worst-case conditions, up to 40% of all predictions were route breaks. The remaining 60% represent false alarms identifying and triggering the replacement of inefficient links.

Without link prediction, packet loss and interruptions cannot be avoided. However, our prediction mechanism is able to avoid 70% of these interruptions, even in this worst-case scenario.

One has to keep in mind that there are numerous situations, which cannot be acquired statistically. For instance, when an intermediate node leaves the route and the prediction function regards one of its hops as suspicious but a neighbouring hop breaks first. In these situations, the update nevertheless rearranges the route and inhibits the route breakage. Hence, the breakage is bypassed but this does not appear in Figs. 13 and 14, since the breakage was expected on a different link.

Our approach to weight the LA steps and to sum up the weightings within a certain period is a very elementary method. The analysis shown confirms

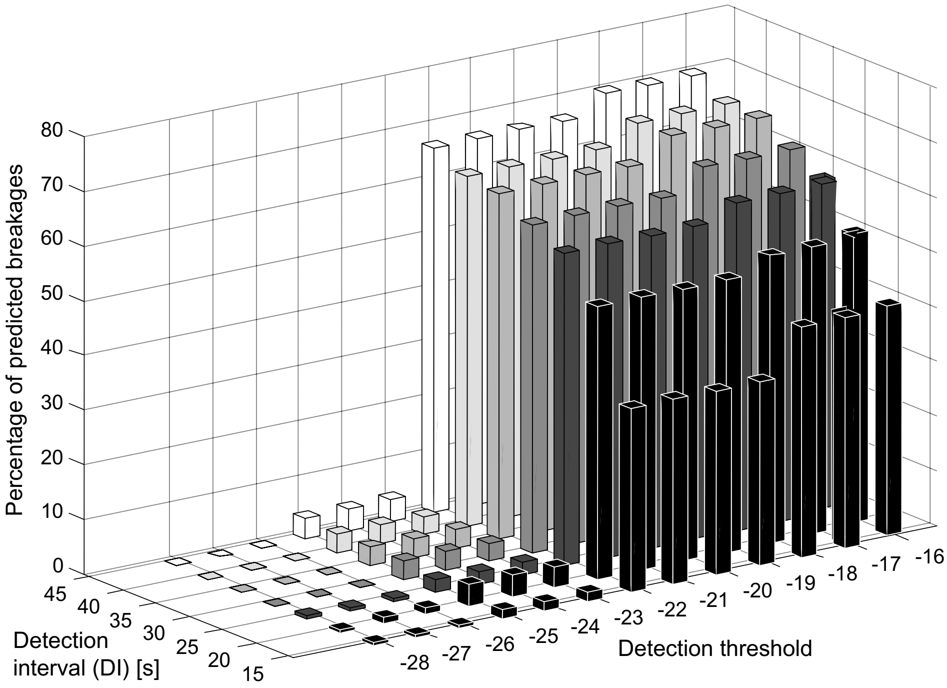

Fig. 13. Percentage of predicted breakages.

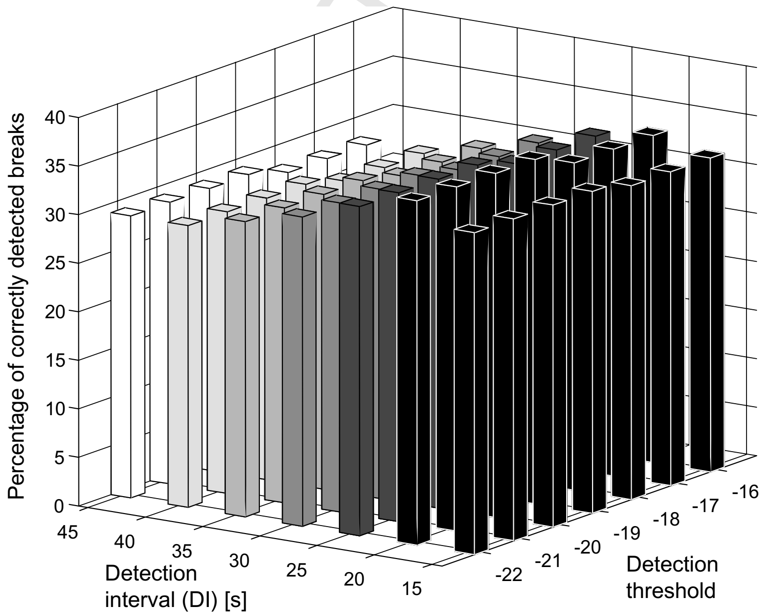

Fig. 14. Percentage of correct detections.

the assumption that a prediction is possible and beneficial. Approaches that are more complex may raise the detection rate of the link breakages.

The detection interval (DI) is chosen according to the node speed and the movement direction. It is very important to select a suited value for the detection interval. However, DI strongly depends on the node speed and therefore cannot be determined in advance. Consequently, we introduce an adaptive windowing approach. Our LA starts to sum up all rating steps during a minimum detection interval (DI_{min}). If the prediction threshold is not exceeded, the window size is enlarged until the upper limit (DI_{max}) is reached. As long as the prediction results do not exceed the detection threshold, no breakage is foreseen. If the threshold is penetrated the network layer is informed that the link might break. The interrelationship between the dynamic detection window, detection threshold and the rating function is expressed in (5.1). Eq. (5.1) sums up different intervals. Each interval starts at a different time in the past ranging from $t\text{-}DI_{min}$ to $t\text{-}DI_{max}$ and ends at the current time. Since switching down is rated negative, the infimum is calculated over all sums. If the infimum falls short of the applied threshold $D_{threshold}$ a link breakage is predicted.

$$D_{threshold} \leqslant \inf_{DI \in [DI_{min}, DI_{max}]} \left(\sum_{t-DI}^{t} RF(t) \right). \quad (5.1)$$

The prediction is not only feasible at the sending node, but also at the receiving node.

Fig. 15 gives an overview of the different functionalities and their ways of cooperation. The LA adapts the PHYModes to operate each link appropriately. The rating function reviews the different LA steps and the prediction function summarises the rating results and determines whether the link is instable or not. In case the link is expected to terminate the route rearrangement algorithm is instructed to look for an alternative route. Thus, the prediction enables the route rearrangement algorithms to circumvent numerous route breakages.

6. Proper actions for upcoming link break

Assuming the link adaptation delivers the necessary information about the link state characteristics, this information triggers appropriate actions either to rescue the link and avoid a route rediscovery or

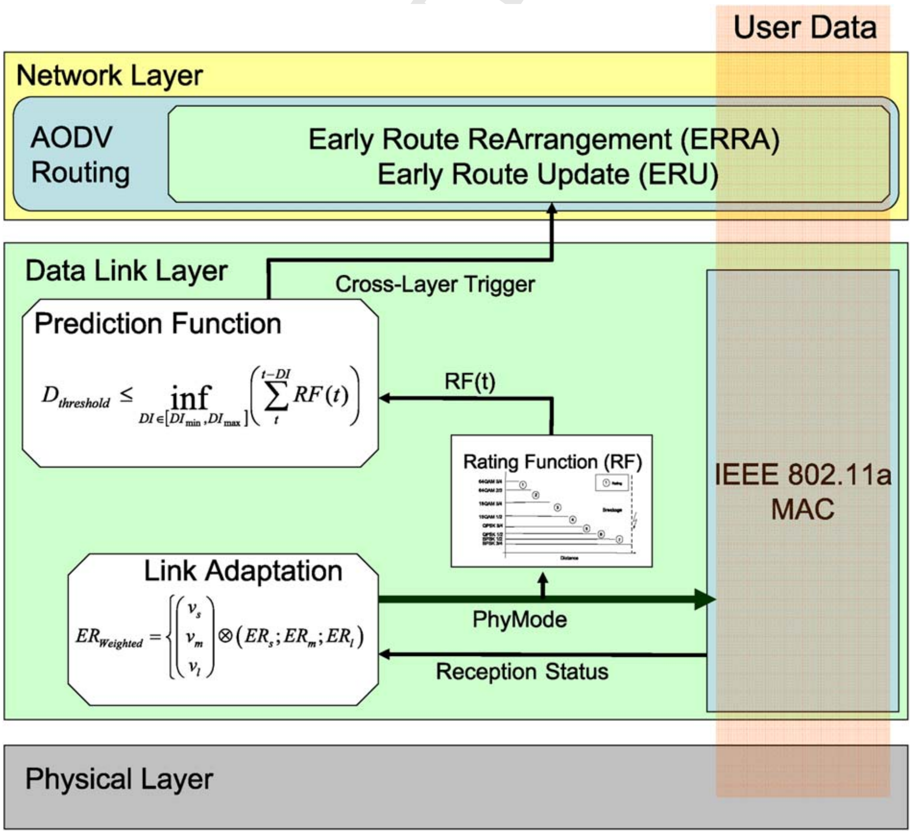

Fig. 15. Cooperation between LA, rating function, prediction and network layer.

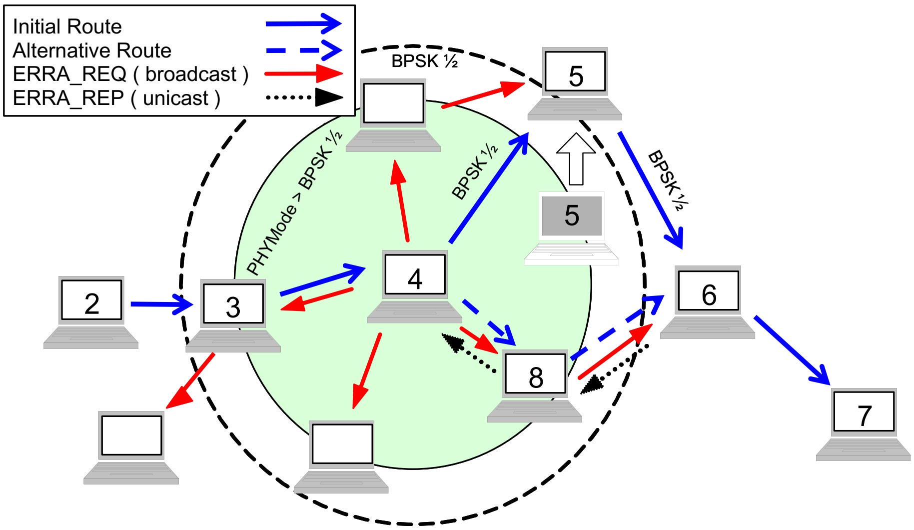

Fig. 16. ERRA signalling.

to provide an improved link quality by finding a new route. In any case, several proper actions are conceivable. The node that monitors incoming and outgoing connections knows if one of these links, none or both of them have changing PHYModes. This enables the node to distinguish three different cases:

1. The node recognizes that the LA for the outgoing link is adapting towards lower transmission modes but the incoming link remains stable. This is a typical situation, where the next node on the route wanders out.
2. The node recognizes that the incoming as well as the outgoing links are adapting towards lower transmission modes. This indicates movement of the node itself. Thus, the node regards itself as an instable intermediate node.
3. The LA for the incoming link has to decrease the PHYModes but the outgoing link remains constant. That is typical for a preceding node moving away.

In the scenario depicted in Fig. 16 all the three cases[3] are presented. Node 4 experiences case 1, node 5 faces case 2 and node 6 is exposed to case 3.

6.1. ERRA: Early Route ReArrangement

In the previous section, we explained how to forecast the degradation of a link. This section describes an approach that profits from early triggering. The Early Route ReArrangement (ERRA) is derived from the local repair idea, which is part of the Ad Hoc on Demand Distance Vector (AODV) routing protocol [4].

Unlike the local repair idea, ERRA does not wait until the link is broken. Prior to a breakage, ERRA rearranges the route to avoid disruption. In Fig. 16 an example is given. The initial route starts from source node 2 to destination node 7. One intermediate node (5) is going to wander off. Node 4 first detects the movement; since it has to adapt the PHYMode for the outgoing link to node 5. Once node 4 uses PHYMode BPSK 1/2 it starts looking for a downstairs-pattern in the elapsed timeframe. If node 4 finds an indication for such a pattern, it triggers the ERRA procedure to rearrange the route.

Node 4 locally broadcasts[4] a rearrangement request (ERRA_REQ) with a PHYMode higher than the last one used for the connection and consequently, reducing the coverage range for the ERRA_REQ (cp. Fig. 2). This ensures that the former link between nodes 4 and 5 is not selected. In

[3] Obviously, the three cases can also occur when the neighbour terminals are moving; however the upcoming situation could be handled equally.

[4] The time to life (TTL) for the broadcast is calculated according the AODV local repair rules [4].

Fig. 16 the request is sent with QPSK 1/2. Therefore, node 5 does not receive the request directly. Node 8 forwards the request to node 6, which is aware of a route to the destination. Node 6 responds (ERRA_REP) and provides the alternative route. Afterwards, node 4 compares the hop counts of the old and the new route. If the new hop count is less or equal, the alternative route is used immediately. Otherwise, node 4 uses the new route immediately after the old connection finally breaks. Further details are depicted in [6]. ERRA rearranges the route to provide robust connections ensuring improved route continuity that is an important requirement for transport protocols. However, there are ways to further improve the mechanism. When a node discovers a degrading link, the connection still exists and can be used for the route update process. Therefore, we extend ERRA and introduce the Early Route Update protocol in the following section.

7. ERU: Early Route Update

To avoid connection interruption the node with a degrading outgoing link negotiates a workaround with the node behind the upcoming breakage. We assume that each node has an up to date list of nodes in its neighbourhood. This is achieved by using hello messages. Figs. 17 and 18 illustrate the ERU signalling: Again, node 5 leaves the transmission range. Node 4 is triggered from its prediction due to the degrading link and adds a list of its neighbouring nodes to an ordinary data packet[5] (ERU_PATCH_INFO) that is received by node 5.

Since node 5 notices via the LA procedure that its incoming and outgoing connection for that particular route is instable, it forwards the information to the next hops. Stable nodes retrieve the list of neighbours attached to the data packet. In this case, node 6 is stable since it has a stable outgoing link. The ERU_PATCH_INFO contains a counter for the number of hops from its source to the current stable node. This counter represents the size of the instable part of the route. We refer to this counter as the breakage hop counter (BHC). Node 6, as the first stable node, searches for an intersection between the received neighbourhood and its own. In Fig. 17 there is no intersection between the set of neighbours. Hence, node 6 broadcasts the list to its neighbours. These forward the list corresponding to the BHC (in our example the info is sent twice). Thus, the broadcast is limited to two hops, reducing the flooding to the vicinity of the disruption. Fig. 18 shows that node 11 knows node 8. Therefore, it is included in the neighbour list. As a result, node 11 creates a reply message (ERU_REP) and sends it to node 4 via node 8. Node 4 applies the same rules for using the new connection as mentioned for ERRA. A detailed description, including some special cases handling, is given in [6].

8. Simulation results

In an approach similar to our statistical evaluation, we present simulation results for the idealised setup shown in Fig. 9[2]. In addition, we investigated the worst-case scenario (see Fig. 11) containing 40 nodes and a movement following the RWP mobility model. The LA algorithm and the cross-layer interaction between LA and IP routing are evaluated by means of simulation. We start with an in deep review of the transient behaviour of the route rearrangement mechanisms compared to standard AODV with local repair.

Fig. 19 shows the LA steps vs. time, for the link between the source node and the next hop neighbour. The simulation shows one entire turn of the circle (compare Fig. 9[2]). The simulation was repeated applying standard AODV, AODV with ERRA and AODV with ERU. The results are presented in Fig. 19 which contains three curves. The first one highlights the LA steps using standard AODV and shows several drawbacks. Primarily it is obvious that the link keeps BPSK 1/2 until the connectivity is finally lost. During this long period the link burdens the network by operating with an inefficient PHYMode to transmit its data. Owing to the fact that BPSK 1/2 is exhaustively used, the opportunity to rearrange the route and to select a better-suited node is missed. Consequently, the route breaks and a certain number of packets is lost and these have to be repeated. The next step is reestablishing the route and choosing an intermediate node, which is already fading away. Therefore, the maximum PHYModes are limited to QPSK 3/4 after the first three breaks. After the fourth route is switched towards transmitting via the incoming nodes (transmitting clockwise). Hence, for a limited time the next node approaches and the link quality increases. Having passed the sender, it fades away

[5] Assuming the IEEE 802.11 maximum packet (2304 Byte) size is not exceeded.

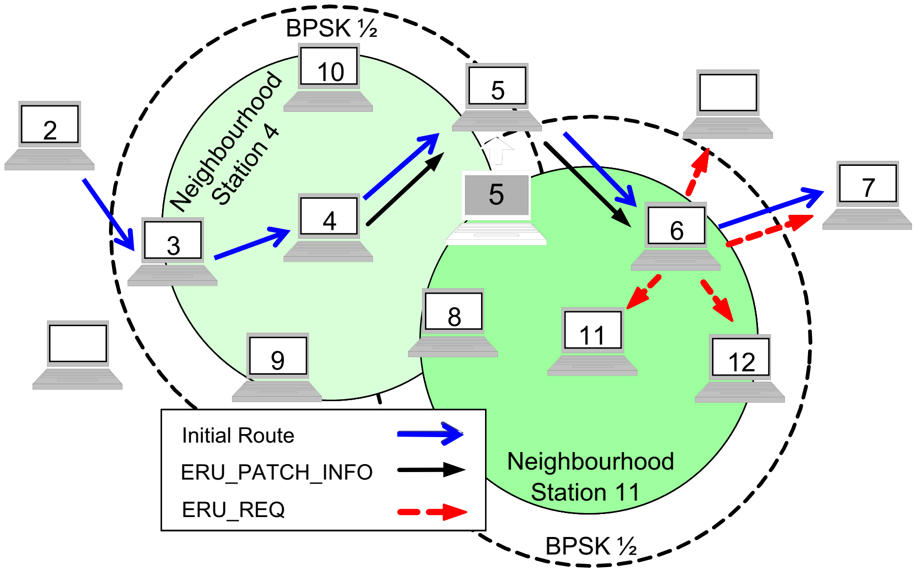

Fig. 17. ERU request signalling.

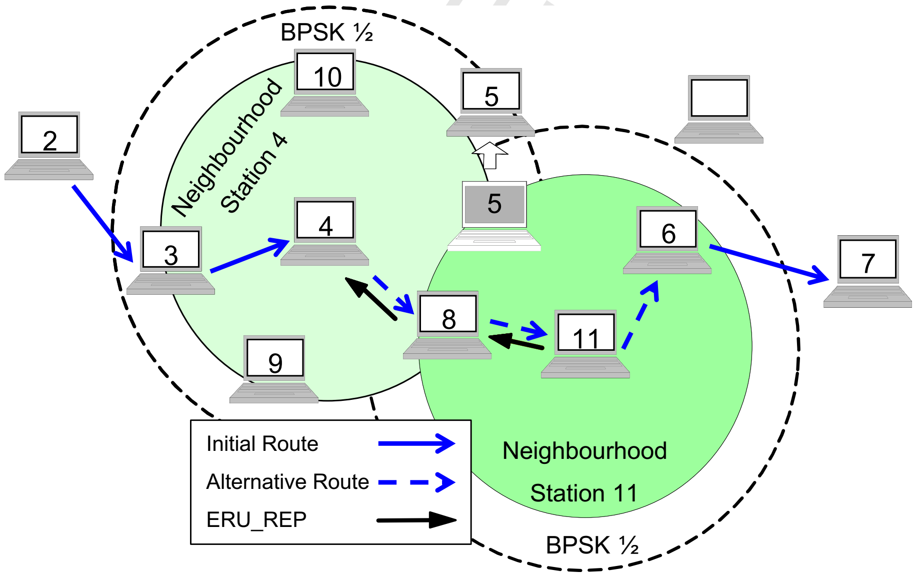

Fig. 18. ERU reply signalling.

again. That describes a typical behaviour found while using most approaches.

The medium curve represents the handling of the situation by ERRA. Immediately after BPSK 1/2 is engaged, the rerouting process is started and ERRA switches to a new route. Adapting the route with ERRA is fast, which results in short peaks towards BPSK 1/2. ERRA lost no packets on the complete turn, implying five route adaptations.

The newly engaged routes are more stable and allow higher PHYModes on the described link. The higher PHYModes shorten the packet transmission time and disburden the network capacity. Similar to situation with AODV, a switch to a

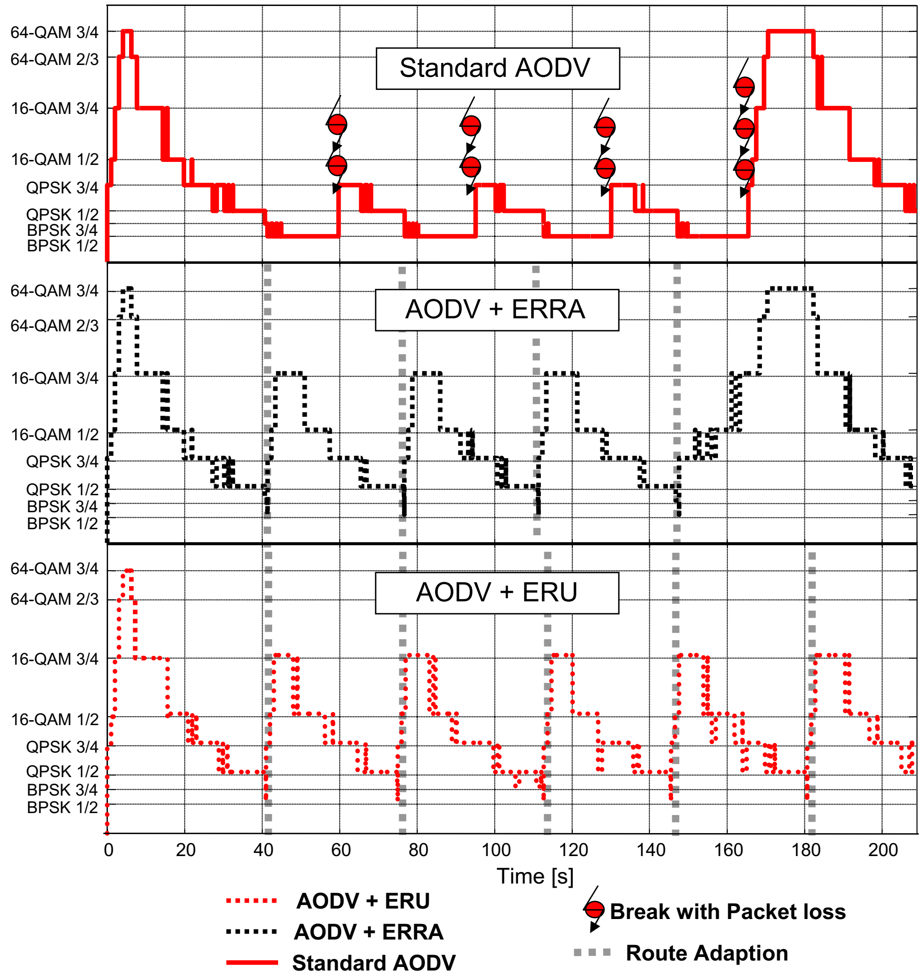

Fig. 19. Comparison of different routing behaviour.

clockwise direction generates increasing link quality due to an approaching next hop partner.

ERUs mechanism is based on locally circumventing the gap. ERU starts adapting the route from the node behind the upcoming breakage. Consequently, the gap is filled by the mechanism with the next available node. Route breaks and packet losses are avoided. The tradeoff for this is increasing route lengths. The route is not switched to a clockwise transmission at the same time like ERRA. When the destination appears, in the neighbourhood of the breakage the initial situation is re-established and the direct route is chosen.

Figs. 20 and 21 highlight the handling of first situation with degrading link quality with AODV and ERRA. Fig. 20 displays the situation after 60 s for AODV. The link finally breaks and two packets are lost. After the break (60 s) node 7 is inserted as new intermediate node, whereas ERRA in Fig. 21 reacts earlier and rearranges after 40 s. The PHYMode curve in Fig. 21 clearly displays the predicted downstair-pattern prior to route switching. We present no detailed figure for ERU because it shows the same fast reaction as ERRA in this situation.

In addition, we show the detailed figures for the situation where AODV and ERRA switch to clockwise routing (see Figs. 22 and 23). Fig. 24 shows that ERU keeps the route direction and fixes the gap locally. Both proposed protocols guarantee the route continuity, forfeit no packets and prevent route breaks.

After discussing the idealised setup, we complete our simulation analysis with the worst-case scenario mention in Section 5 and displayed in Fig. 11.

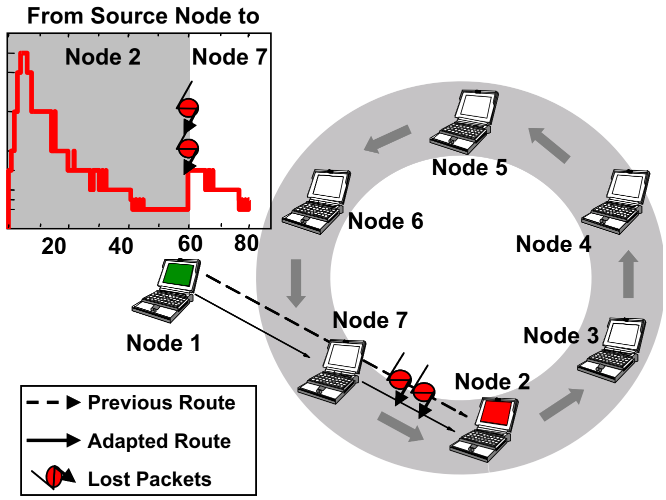

Fig. 20. AODV handles the first situation with degrading link quality.

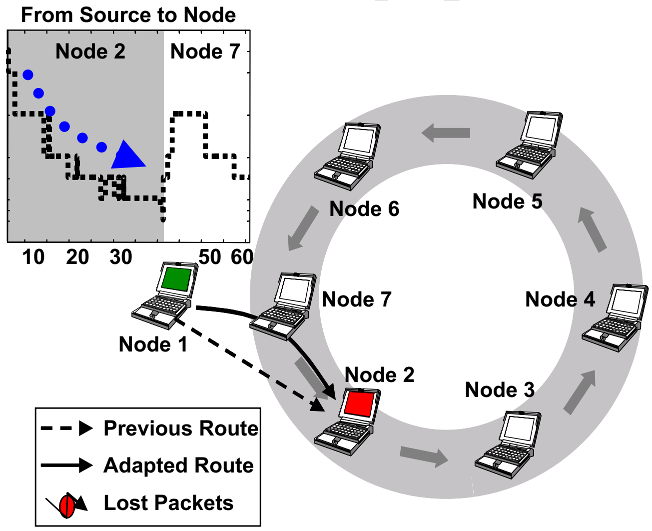

Fig. 21. ERRA handles the first situation with degrading link quality.

Three routes are loaded with constant-bit-rate traffic. The offered traffic increases with every simulation. The packet size is set to 512 B. RTS/CTS handshake is used to reduce the hidden node problem. Fig. 25 presents the percentage of average throughput over all three routes. The figure compares ERRA and ERU with the AODV local repair mechanism. Generally, under high load conditions, the network is congested and cannot deliver all packets. It is important to see in Fig. 25 that no throughput degradation occurs using the ERRA or ERU algorithms. This is because packets are only affected, if a breakage situation is foreseen. Thus, both approaches only delay a small fraction of packets.

In terms of additional signalling overhead ERRA and ERU are comparably efficient with local repair from AODV. ERRA uses the same amount of signals and bytes per signal as local repair. However, ERRA redirects the route in advance and disburdens the channel, by choosing a higher PHYMode for signalling, thus producing shorter packets.

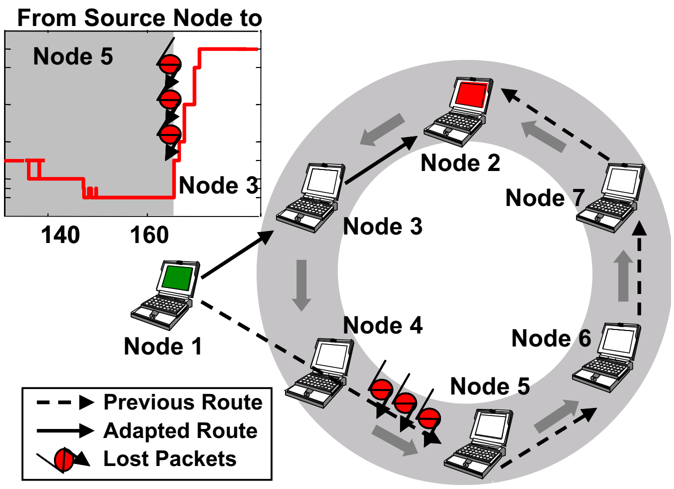

Fig. 22. AODV handles fourth route break.

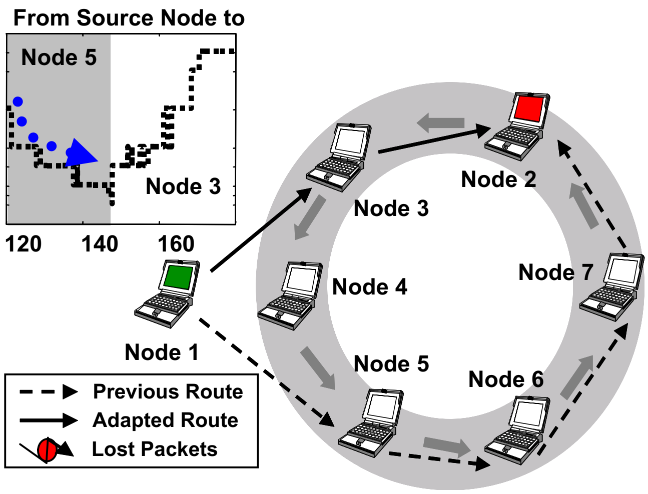

Fig. 23. Fourth route adaptation by ERRA.

ERU requires knowledge about the actual neighbourhood. As proposed by AODV [4] as an optional feature, nodes learn the neighbourhood using hello messages. Hello messages increase the signalling overhead, but enable ERU to smoothly adapt the routes and avoid breakages. ERRA and ERU perform beneficially unless the network is uncongested, which represents the usual case. As soon as the network cannot carry the offered traffic, routes break and the user satisfaction decreases. Neither of the two approaches can improve the situation. However, both do not worsen the situation. Under overload conditions, ERRA and ERU perform similar to local repair. Figs. 25 and 27 lead to the same conclusions.

Fig. 26 presents the packet delay for all three routes. It shows the results for both proposed approaches in comparison with the AODV local repair procedure.

Apart from the typical delay characteristics originated from the reactive routing protocol, it is obvious that both approaches outperform the AODV local repair mechanism. When the offered traffic increases, ERRA and ERU reveal the same performance as local repair. The involved signalling does not negatively influence the throughput (cf. Fig. 25).

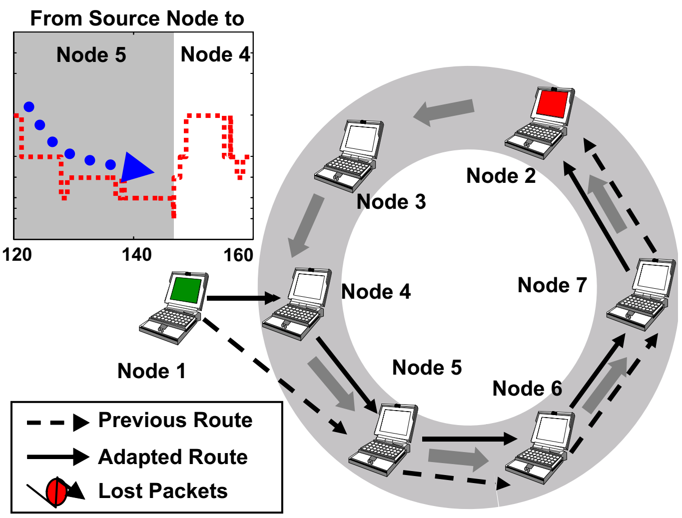

Fig. 24. Fourth route adaptation by ERU.

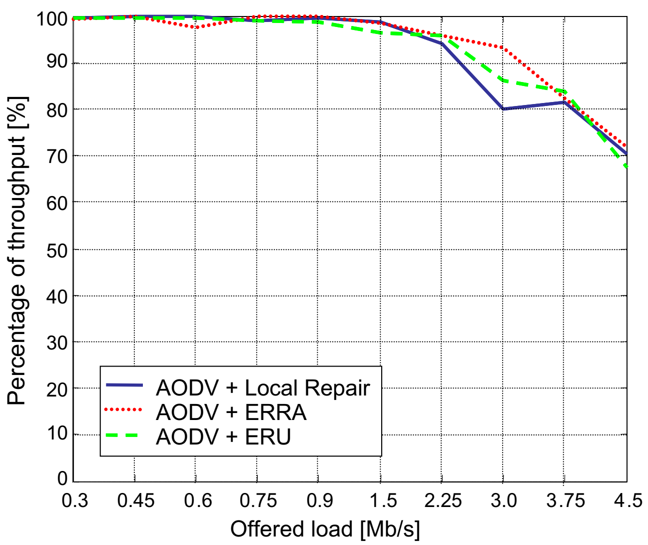

Fig. 25. Throughput percentage.

Under low load conditions, ERU shows the lowest delay. With the increase of the traffic load ERRA and ERU still achieve smaller delay than local repair (cf. Fig. 27). We can conclude that link prediction improves the route continuity, avoids packet losses, and decreases packet delay because of the timely and accelerated route discovery procedures.

9. Conclusions

This article explains the Early Route ReArrangement (ERRA) and the Early Route Update (ERU) approaches based on link breakage prediction. We present the idea to predict the link state based upon the link adaptation behaviour. We describe a suitable link adaptation (LA) and show its functionality. Based on link adaptation, we introduced a prediction algorithm that rates the PHYMode changes in terms of their importance towards an upcoming route interruption. The prediction enables our route rearrangement protocols to act timely and prevent route breaks and packet losses. In particular, ERRA and ERU are designed to benefit by being triggered early from prediction algorithms, acting early enables shorter and more

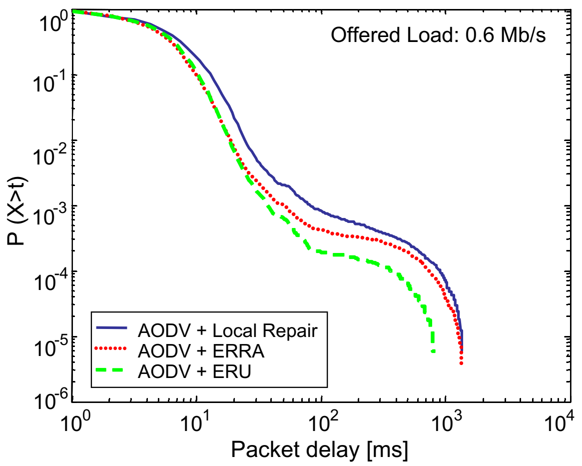

Fig. 26. Complementary cumulative distribution function (CCDF) of the packet delay.

stable routes. Better PHYModes result in shorter packet and less transmission duration, thus reducing network congestion and disburdening network capacity. Higher layer transport protocols noticeably benefit from reduced packet loss and route breaks.

This article presents an efficient control loop based upon cross-layer information shared between medium access and network layer. Thereby, this article gives a first glimpse to the potentials of cross-layer interaction.

10. Discussion

Evidently, our LA algorithm presented here cannot distinguish between packet loss originated from transmission errors or collisions. In a congested channel, the LA procedure detects unacknowledged packets and decreases the PHYMode. However, this increases packet transmission time and worsens the situation. In the scenarios described here, this behaviour is unfavourable. In contrast, our current

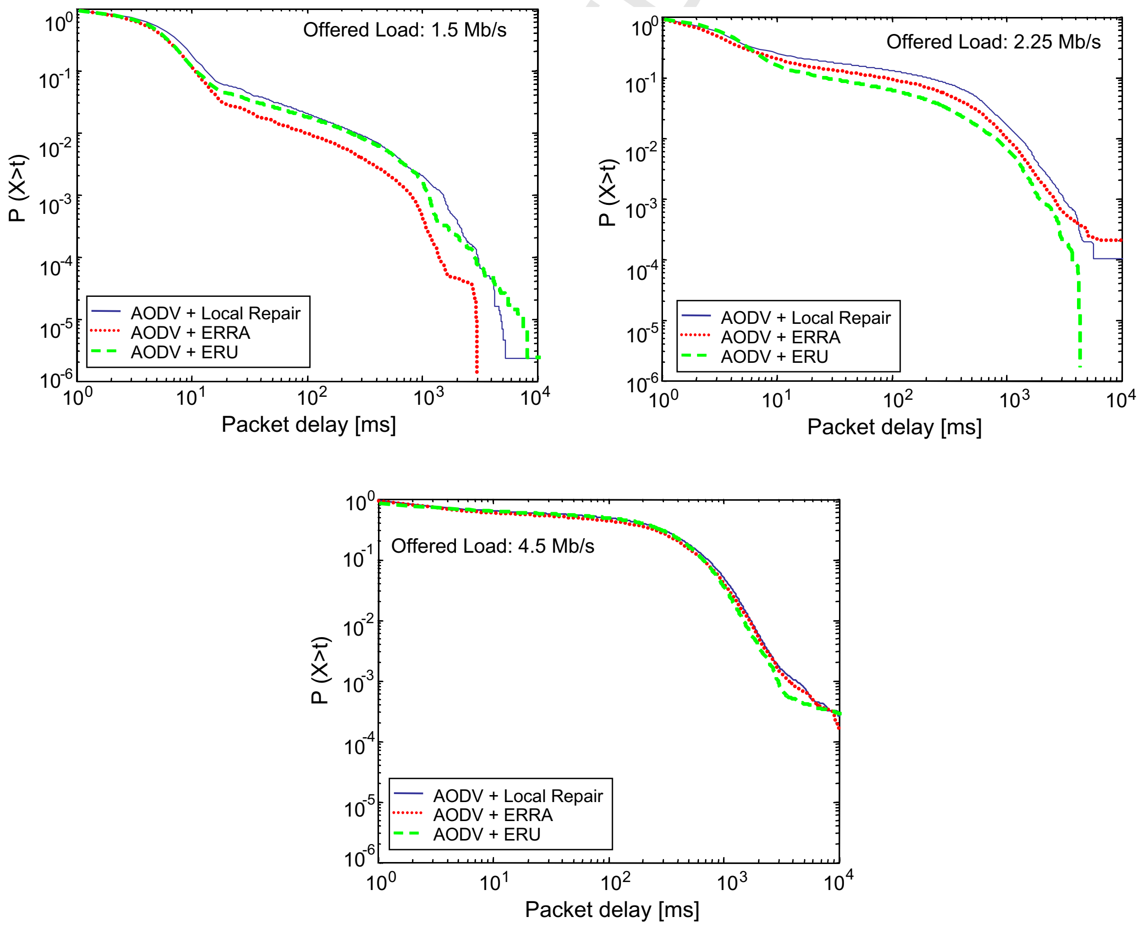

Fig. 27. Packet delay (CCDF) for an increased traffic offer.

work monitors the MAC queue length and enhances the LA efficiency thereby. If the channel busy time increases, monitoring MAC transmission queues reveals that congestion is more probable. Therefore, the LA algorithm decisions could be improved with MAC queue length information taken into account. While our current LA algorithm will not increase the PHYMode in case the channel is congested, an enhanced LA might advise to do so. With increased PHYMode, congestion could be reduced. Congested links using the fastest PHYMode need to detect and establish new routes around the local congestion.

11. Uncited references

[5,8,14].

Acknowledgements

This work was supported by T-Systems, Deutsche Telekom and the German research project IPonAir, funded by the German Federal Ministry of Education and Research. The authors would like to thank the members of the project for the valuable discussion. The contributions of our colleague Michael Fuhrmann are highly appreciated.

References

[1] B. Walke, Mobile Radio Networks, first ed., Wiley, New York, 1999.
[2] T. Goff, N.B. Abu-Ghazaleh, D.S. Phatak, R. Kahvecioglu, Preemptive routing in ad hoc networks, in: Proceedings of ACM/IEEE MobiCom, July 2001, pp. 43–52.
[3] IEEE LAN/WAN Standards Committee, Part11: Wireless LAN Medium Access Control (MAC) and physical layer (PHY) specifications: high-speed physical layer in 5 GHz band, IEEE Std 802.11a-1999, IEEE, New York, November 1999.
[4] C. Perkins, E. Belding-Royer, S. Das, Ad hoc on-demand distance vector (AODV) routing, RFC 3561, IETF Network Working Group, July 2003, Category: Experimental.
[5] C.E. Perkins, Ad Hoc Networks, Addison-Wesley, New York, 2000.
[6] E. Weiss, M. Frewel, B. Xu, G. Hiertz, Improving ad hoc routing for future wireless multihop networks, in: Proceeding of European Wireless 2004, Barcelona, Spain, February 2003.
[7] C. Bettstetter, H. Hartenstein, X. Pérez-Costa, Stochastic properties of the random waypoint mobility model, in: ACM/Kluwer Wireless Network, Modelling and Analysis of Mobile Networks, March 2003 (special issue).
[8] E. Weiss, G. Hiertz, S. Hischke, B. Xu, Performance analysis of AODV on top of IEEE 802.11a and the impact of the 5 GHz channel, in: Proceedings of Wireless 2003, Calgary, Canada, July 2003.
[9] A. Kamerman, L. Moneban, A high-performance wireless LAN for the unlicensed band, in: WaveLAN II, Bell Labs Technical Journal (1997) 118–133.
[10] G. Holland, N.H. Vaidya, P. Bahl, A rate-adaptive MAC protocol for multi-hop wireless networks, in: Mobile Computing and Networking, 2001, pp. 236–251.
[11] B. Sadeghi, V. Kanodia, A. Sabharwal, E. Knightly, Opportunistic media access for multirate ad hoc networks, in: Mobicom 2002, September 2002.
[12] S. Mangold, S. Choi, N. Esseling, An error model for radio transmissions of wireless LANs at 5 GHz, in: Proc. Aachen Symposium, 2001, pp. 209–214.
[13] J. Khun-Jush, P. Schramm, U. Wachsmann, F. Wenger, Structure and performance of the HIPERLAN/2 physical layer, in: Proc. IEEE VTC Fall-1999, Amsterdam, The Netherlands, September 1999, pp. 2667–2671.
[14] Chair of Communication Networks, RWTH Aachen University, Kopernikusstraße 16, 52074 Aachen, Federal Republic of Germany. Available from: <http://www.comnets.rwth-aachen.de>.
[15] C.E. Perkins, Pravin Bhagwat, Highly dynamic destination-sequenced distance vector routing (DSDV) for mobile computers, in: Proc. SIGCOM'94 Conference on Communication Architectures, Protocols and Applications, August 1994, pp. 234–244.
[16] S. Murthy, J.J. Garcia-Luna-Aceves, An efficient routing protocol for wireless networks, in: Routing in Mobile Communication Networks, ACM Mobile Networks and Applications Journal (1996) (special issue).
[17] D.B. Johnson, D.A. Malz, Yih-Chun, The dynamic source routing protocol for mobile ad hoc networks (DSR), IETF Internet Draft, draft-ietf-manet-dsr-10.txt, in preparation.
[18] Z. Haas, M. Pearlman, The performance of query control schemes for the zone routing protocol, in: Proc. SIGCOMM'98 Conference on Communications Architectures, Protocols and Applications, September 1998.

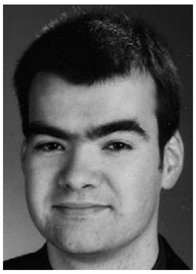

Erik P. Weiss received his diploma degree in Electrical Engineering from Aachen University, RWTH, Germany, in 2001. After his studies he joined the Chair of Communication Networks (ComNets) at RWTH Aachen University, where he is working towards his PhD degree. He participates in the IPonAir project in cooperation with T-Systems. His working areas are the integration of heterogeneous systems, IP mobility, Cross-Layer Communication, and Routing in Ad Hoc Network. His current research interests are the development of a common inter-system architecture, performance analysis of vertical handover mechanisms between GSM/GPRS/UMTS and IEEE 802.11a/g/b. At present he is involved in the European project MYCAREVENT for vehicular diagnosis and maintenance and leads the work package for mobile communication (WP4). He is a student member of IEEE, inventor/co-inventor of several patents and has authored/co-authored several papers at IEEE conferences.

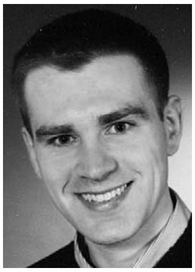

Guido R. Hiertz studied electrical engineering at RWTH Aachen University. During his studies he focused on communication networks, computer science and engineering. In his diploma thesis (MS) he included 802.11e functionality in an advanced simulation tool and surveyed QoS supporting procedures. Since April 2002 he is with the Chair of Communication Networks (ComNets) at RWTH Aachen University, working towards his PhD. His main research fields are support for QoS WLAN (802.11e), protocols for Gigabit (802.11n) and Mesh wireless LAN (802.11s) and PAN (802.15.5). He has been involved in and the editor of different research projects. At present, he is involved in the research project Wireless Gigabit with advanced Multimedia support (WIGWAM) that is funded by the German Federal Ministry of Education and Research. He has been involved in the design of the high speed WPAN MAC protocol of WiMedia Alliance that became ECMA standard in 2005. Since 2004 he is a voting member of IEEE 802.11, where he submitted several presentations and proposals. He is charter member of Wi-Mesh Alliance that submitted a joint proposal to 802.11s. He is the inventor/co-inventor of several patents. As student member of IEEE, he has authored/co-authored several papers at IEEE conferences.

Bangnan Xu received his BSc and MSc degrees in electrical engineering from Dalian Maritime University, Dalian, China in 1986 and 1989, and PhD (Dr.-Ing.) degree in information technology from Aachen university of Technology in 2002, respectively. From 1996 to 2001, he was a research assistant at the chair of communication networks, Prof. Dr.-Ing. B. Walke, Aachen University of Technology. Since 2001, he has been with T-Systems, Deutsche Telekom, working as R&D Fellow and Project manager in the department of Mobile and Wireless Solutions.

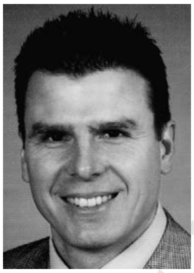

Sven Hischke received the diploma degree in Electrical Engineering from the University of Applied Sciences Giessen-Friedberg and the PhD degree from City University London in 1996 and 1999, respectively. From 1999 to 2003 he was with T-Systems in Darmstadt where he was responsible for different research projects in the area of broadband wireless systems and mobile networks focusing on the design of IP-based architectures. In October 2003 he joined the corporate innovation department of Deutsche Telekom as a R&D program manager for broadband wireless access and global seamless network projects. Since May 2005 he is a senior manager innovation management of Deutsche Telekom and is working on the identification and development of group wide products and business models in the area of seamless services.

Bernhard H. Walke is running the Chair for Communication Networks (ComNets) at RWTH Aachen University, Germany, where about 30 researchers work on topics like air-interface design, development of tools for stochastic event driven simulation and analytical performance evaluation of services and protocols of XG wireless systems. Most of this work continuously has been funded from third parties' grants. He is author of the 2002 book "Mobile Radio Networks – Networking, Protocols and Traffic Performance" and co-author of the 2001 book UMTS – The Fundamentals and the forthcoming 2006 book "IEEE 802 Wireless LAN/PAN/MAN Systems: Standards, Models and Traffic Performance". He has been a board member of ITG/VDE and is Senior Member of IEEE. He has served as Programme Committee and Steering Committee Chair of various conferences like the European Wireless (EW) conference that he co-founded. In 2005, he was the Scientific Chair of IEEE-PIMRC 2005, Berlin. His group has substantially contributed to the development of standards like ETSI/GPRS, ETSI/BRAN HiperLAN2, CEN TC 278 DSRC (electronic fee collection), IEEE 802.11e, 802.16 and 802.15.3. From 2001 to 2003 he was an elected Chair of Working Group 4 (New Technologies) of the Wireless World Research Forum. Prior to joining academia, he worked for 18 years in various industry positions at AEG Telefunken (now EADS AG). He holds a Dr. degree (1975) in information engineering from University of Stuttgart, Germany.

Sebastian Gross studies towards his diploma degree in Electrical Engineering at the RWTH Aachen University. He has taken a strong interest in wireless communication and networking. After finishing his student thesis at the Chair of Communication Networks at RWTH Aachen University, he plans to write a diploma thesis in the field of wireless communication networks.